Werk

Jahr: 1977
Kollektion: fid.geo
Signatur: 8 Z NAT 2148:44
Digitalisiert: Niedersächsische Staats- und Universitätsbibliothek Göttingen
Werk Id: PPN1015067948_0044
PURL: http://resolver.sub.uni-goettingen.de/purl?PPN1015067948_0044

LOG Id: LOG_0019
LOG Titel: Payload BI: A compact and economic d-region experiment package for use on small sounding rockets
LOG Typ: article

Übergeordnetes Werk

Werk Id: PPN1015067948
PURL: http://resolver.sub.uni-goettingen.de/purl?PPN1015067948
OPAC: http://opac.sub.uni-goettingen.de/DB=1/PPN?PPN=1015067948

Contact

Niedersächsische Staats- und Universitätsbibliothek Göttingen
Georg-August-Universität Göttingen
Platz der Göttinger Sieben 1
37073 Göttingen
Germany
Email: gdz@sub.uni-goettingen.de

J. Geophys. 44, 65–79, 1977

Journal of Geophysics

Payload BI: A Compact and Economic D-Region Experiment Package for Use on Small Sounding Rockets

G. Rose and H.U. Widdel

Max-Planck-Institut für Aeronomie, D-3411 Katlenburg-Lindau 3, Federal Republic of Germany

Abstract. A payload is described consisting of a foil cloud experiment and a guard ring probe. Winds, wind shears and turbulent motions are derived from the spatial movement of the cloud during fall and density and temperature of the neutral air from the fall rates of the cloud, as observed by radar respectively. Electron and ion densities are measured by a guard ring probe of special design. The probe is calibrated by comparison with the results of simultaneous ground based measurements of radio wave absorption applying the Sen-Wyller formula. The set up of the payload and its operation are described and some results are given.

Key words: D-region – Winter anomaly – Wind – Air density – Electron ion density – Falling foil cloud – Guard ring probe.

Concept of BI Payload

Payload BI was designed to gather an overview over the time history of changes of atmospheric parameters in the D-region which comprise both changes in the ionized components and of neutral air (meteorological) parameters.

A fairly large number of individual experiments are required for such a project in order to achieve a significant result. Cost-effectiveness and reliability of the payload are of utmost importance but not at the expense of scientific value or accuracy of measurement. A careful consideration about parameters to be measured is mandatory. The payload to be described here contains two experiments, one for the measurement of neutral air parameters, the other for the measurement of the ionized component of the atmosphere.

The payload was flown successfully a number of times before it was used in the Aeronomy Program (Rose and Widdel, 1972b; Rose et al., 1974; Dieminger et al., 1974).

1. Neutral Atmosphere Parameters: The Foil Cloud Experiment

1.1. Winds, Wind Shears, Turbulent Motions. Winds, wind shears, density and average air temperature can be measured in the simplest way by free-falling, reflective objects which are ejected from the vehicle at or near apogee of the rocket's trajectory and tracked from the ground by suitable means, e.g. radars. Such an experiment has the "all-weather" capability desired for this type of investigation.

Wind measurements allow within certain limits the estimate of large-scale pressure gradients, and, by this, the position of high- and low pressure systems. When temperature measurements are available, wind shears can be used to prove the existence of turbulent layers (Zimmerman and Narcisi, 1970).

For wind measurements, falling spheres of various kinds (Jones, 1959; Otterman, 1961) are not very well suited to greater heights because they are too heavy and their descend velocity is too large to follow the wind shears sufficiently fast (Fig. 1). A more suitable target is a cloud of radar-reflective dipole elements ("CHAFF" or "WINDOW"). Experiments of this kind have been used in the upper atmosphere (D-region heights) by several authors (e.g. Webb, 1961; Smith, 1960; Pachomov, 1969) and also on a routine basis. Rapp (1960) gave an estimate about the accuracy of such experiments.

The main disadvantage of "CHAFF" measurements is the limited height range over which useful measurements can be performed because the cloud spreads out under the influence of diffusion and the initial momentum received during deployment from the spinning rocket. Further, spreading in strong wind shears causes the radar to "hunt". Attempts to overcome this difficulty by using more than one "CHAFF" ejection over the rocket's trajectory have been made by several authors (e.g. Pachomov, 1969). We flew an experimental payload of this kind in 1973 in order to test the feasability of increasing the height range over which density measurements can be made.

Ordinary "CHAFF" has also a very strong tendency to form clumps because the very thin, hair-like dipole elements do not separate well. This tendency is almost impossible to avoid as our own tests and those of other experimenters have shown. This makes the derivation of air densities and air temperatures from fall rates of "ordinary" CHAFF clouds almost impossible (very rare cases excepted).

However, when elements of proper shape and suitable size and wing load area to have little tendency to form clumps are chosen (Rose and Widdel, 1972, 1973) and means are taken to deploy the cloud in such a (controlled) way that the elements are all separated from each other and that their number density increases toward the center of the cloud (Azcarraga, et al., 1970; Rose, et al., 1972), the situation is different and a larger height interval can be covered with reliable measurements provided that no excessive windshears and turbulences are present: These distort the shape of the cloud to such a extent that a reasonably accurate radar track is no longer possible after the cloud has passed the shear (see Fig. 2). This happens with preference at height levels from which so-called "DEEP ECHOES" (Dieminger and Hoffmann-Heyden, 1952; Gregory, 1961; Thitheridge, 1962) are received. A connection between

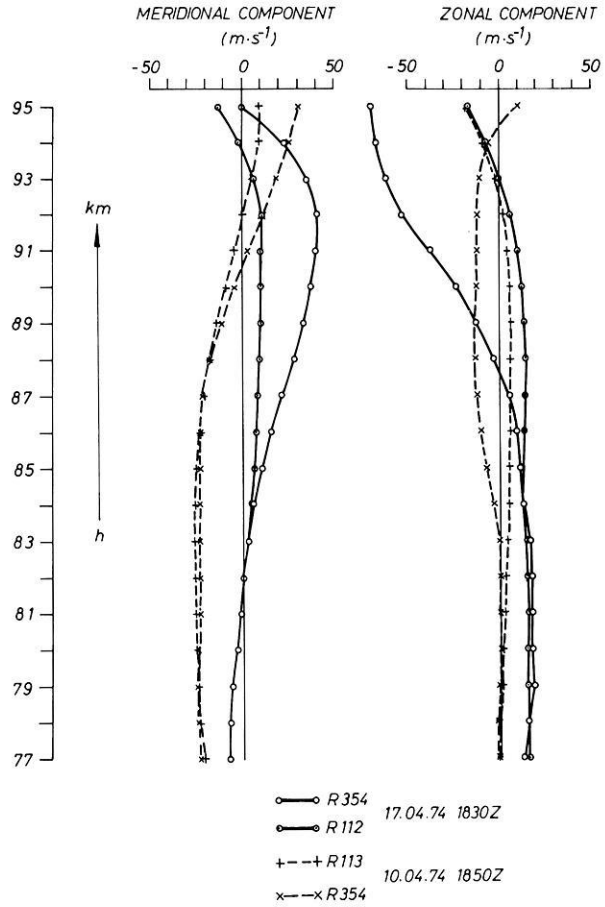

Fig. 1. Response of a falling sphere to winds. Results of tracking by two independent radars

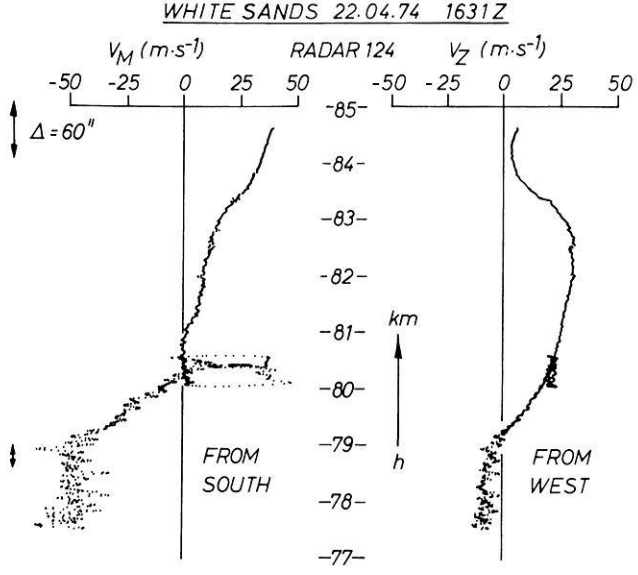

Fig. 2. Results of tracking of a foil cloud passing through a wind shear

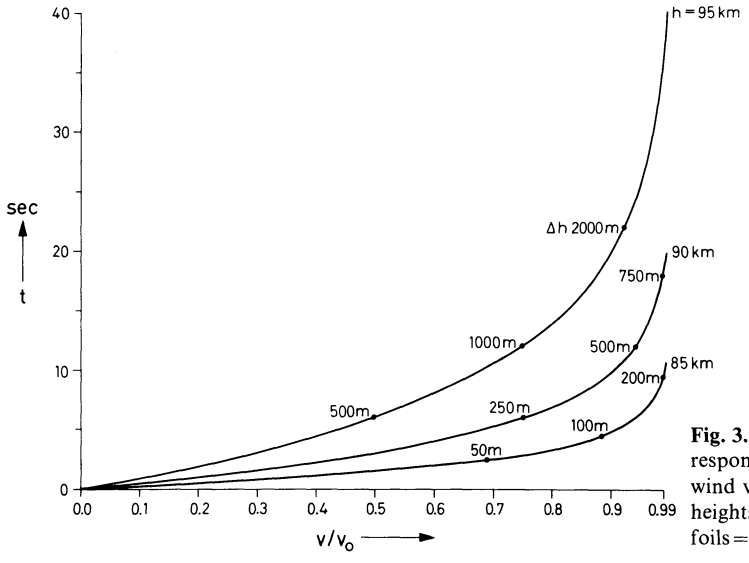

Fig. 3. Calculated response of foil cloud to wind velocity in different heights (initial velocity of foils = 0)

these gradient-induced partial reflections and wind shears seems to be evident though not fully proven by experiments so far.

Even small-scale vertical movements can be observed directly with properly designed foil clouds (Rose and Widdel, 1969) but because these movements are associated with a rapid dissolution of the foil cloud inside the turbulence cell, a fairly sensitive radar is required for tracking. The situation may change when active transponder elements rather than passive reflectors can be used as targets. More detailed investigations of turbulent motions besides wind and density measurements are then possible.

The upper height limit for wind measurement is set by the weight-to-area-ratio of the dipole elements. We use foils, $2.5 \cdot 10^{-6}$ m thick, $9 \cdot 10^{-3}$ m wide, their length cut to be in resonance with the wave length of the radar tracking system. The foils are aluminized from all sides, the weight-to-area-ratio is $3.4 \cdot 10^{-3}$ kg·m^{-1}. These foils have less tendency for "bird's nesting". They allow reliable wind measurements from about 95 km downwards. The foil clouds are deployed near apogee of the rocket's trajectory in the direction opposite to flight. This allows a certain amount of compensation of the trajectory speed. Experience has shown that the clouds deployed this way follow almost immediately the direction of the wind with no discernible "ballistic" component. The theoretical response of the cloud to winds is shown in Figure 3.

One weak point however has to be mentioned. In-situ measurements (of any kind whatsoever) can provide only a momentary picture of the state of the wind field even though it takes 20–25 min for the foil cloud to travel down from 95 km to 80 km. Therefore, tides and waves cannot be separated from the prevailing wind except for the case when a whole series of rocket launches is performed over the day (Azcarraga et al., 1971). In our special case however,

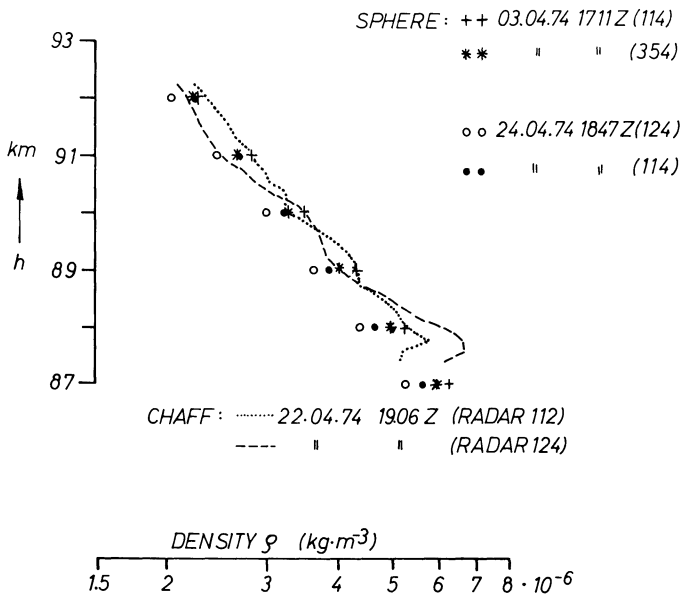

Fig. 4. Density measurement. Comparison between the results attained with falling spheres and with the foil cloud experiment. Each experiment was tracked by two independent radars

in which the winter anomaly is to be investigated, this deficiency is of no significant importance.

1.2. Air Density and Temperature. Air density can be derived from the fall rates of the foil cloud when accurate tracking data are available (Rose and Widdel, 1972) but only over the height range for which the dimensions of the sensor elements (area load and width) are matched to yield low Reynolds numbers and their width is small compared with the mean free path. When the transition region is reached, the increase in density nearly compensates for the decrease of effective drag coefficient and the descend speed of the elements varies then only slowly with height. To restore the flow conditions under which it is possible to derive density one has to match the physical properties of the sensor elements to the relevant height region. Below about 65–60 km the useful height range over which density measurements can be made with "CHAFF" becomes so small that it is of no more practical use, and the method finds its natural limitation (Rose and Widdel, 1972).

This method is sensitive enough to follow diurnal changes of density. From these, even slow vertical movements of the atmosphere can be derived (Azcarraga, et al., 1971; Rose et al., 1972a). Reasonably good agreement between densities derived from falling sphere experiments and foil cloud experiments (Rose et al., 1976) was attained (Fig. 4).

Temperature values can also be derived from the data but only as averages. The second derivative of the data necessary for temperature determination introduces a comparatively large error bar for the temperatures and does not allow at present a finer analysis.

2. Ionized Constituents: The Guard Ring Probe

For the measurement of the ionized component of the D-region atmosphere we used a guard ring probe at the tip of the rocket (Rose et al., 1972b). This probe allows us to distinguish between ions and electrons. Probes of similar design have been used in the past on rockets by several authors, L.G. Smith (1967, 1969) being the first.

While the technical design of the probe itself can be held rather simple, the direct interpretation of the results in terms of absolute values poses a lot of problems. To circumvent these, it has become standard (Thrane, 1974) to calibrate the probe readings against the results of an independent wave propagation experiment flown on the same payload as was first done by Mechtly (Mechtly et al., 1967; Mechtly and Shirke, 1968; Sechrist et al., 1969; Mechtly, 1974). Mechtly found that the "Langmuir" probe readings are proportional to electron concentration up to about 85 km, and tend to deviate from proportionality above this region.

Instead of flying simultaneously an independent wave propagation experiment on each payload for calibration purposes, we used a different approach to convert the probe data into ambient electron densities. We used the results of the ground-based absolute absorption measurements and ionosonde data and results of our in-situ density measurements which have to be performed anyway when such investigations are made.

Our variant of the probe was based upon experience gained during the development of a parachute Gerdien-type experiment (Widdel, et al., 1971; Borchers, 1971; Widdel et al., 1977). We found that insulator surfaces can have an important detrimental effect upon the stability of the zero point especially when the probe potential is changed, because these surfaces collect charges preferably of one polarity because the accommodation coefficients are different. This effect disappears when the insulator is kept as small as possible and recessed.

The insulator of our probe is recessed by about 5 mm in a gap between body and probe tip, only 0.5 to 1 mm wide. The corresponding increase in capacity was compensated by a rather large guard ring section held always on the same potential as the measuring nose tip. The current/voltage characteristics were then what one would expect from the mobility concept. Electrons are easily distinguished from ions because their mobility is so much higher. The probe resembles more an "open" Gerdien mobility probe aspiration system than a "Langmuir" probe. The regime in which the probe operates is easily seen because a time-linear, triangle-shaped waveform and linear amplifiers are used.

Because wake effects can play an important role (as was outlined by Smith) a stable flight behaviour of the rocket is mandatory. This condition was met by selecting a suitable rocket (SKUA II) and each payload was carefully balanced before flight by moment and couple.

2.1. Probe Calibration Procedure. The ground-based data yield the total absorption L_{TOT} measured on an absolute scale over an A_3 absorption path which is always propagated via the $1 \times E$ hop mode during daytime. (Rose and Widdel,

1977a). The reflection height $h'_E(f)$ is taken from ionograms produced on the range. The foil cloud experiment flown on the same rocket yields the air pressure from which the electron collisional frequency is derived (Phelps and Pack, 1959).

The electron currents I of the probe are assumed to be proportional to the ambient electron densities ($N_e = C \cdot I$, $h < h_o$) up to a height h_o where the mean free path equals the (mean) diameter of the probe. Above that height h_o a correction factor exp (α ($h - h_o$)) is assumed ($N_e = C \cdot I \; exp \; \alpha \; (h - h_o)$) which is replaced by 1 below h_o. The transmission curve technique is applied to the relevant ionograms taken before, during and after the rocket flight with regard to distance and frequency to determine the angle of incidence φ_o into the ionosphere for the A_3 transmission path to the receiver at the launch site. Some well-known approximations are accepted for a moment. The constants C and α which relate the probe currents to the electron densities are then computed in the following way: Starting with the given angle of incidence and an initial pair of constants C and α, a ray-tracing is performed to adjust α in a way that the ray is "homed in" (it just spans then the distance from the transmitter to the receiver). The absorption of the measured ordinary ray is then integrated along this ray path, taking now into account the magnetic field of the earth and using the full Sen-Wyller formulas with the electron collisional frequencies derived from the air pressures. If the absorption thus integrated does not yet fit the experimental A_3 measurements, the constant C is changed a little into the required direction and the calculation is repeated from the very beginning until transmission path and absorption satisfy the experimental data. It should be mentioned that the experimental electron current profiles were replaced close to the (final) reflection level by an equivalent exponential profile (or they were extrapolated exponentially where necessary) in order to determine analytically the curvature of the ray path necessary for the estimations in the vicinity of the reflection level. Experience gained during the aeronomy program has shown that profiles derived in this way from guard ring probe measurements agree reasonably well with those measured by wave propagation experiments.

3. The Payload

Both experiments, the foil cloud experiment and the guard ring probe were matched together in a single payload. Figure 5a shows what the payload looks like and Figure 5b shows a cross section through it. The cylindrical part of the payload contains the foil cloud experiment and the telemetry antennas for data transmission on 235 MHz. The antennas are of the 'traveling-wave" type. The transmitter is located in a bay of the upper part of the payload structure, not far away from the subcarrier oscillators and from the electrometer for the guard ring probe. The latter is housed in a separate cylindrical box for electrical shielding and thermal protection.

Transfer of aerodynamic heat into the payload can be a serious problem. It is more difficult to prevent on small vehicles than on large ones. We solved this problem by avoiding mechanical contact between the inner surface of the nose cone section and the payload structure. The only connection to the metallic

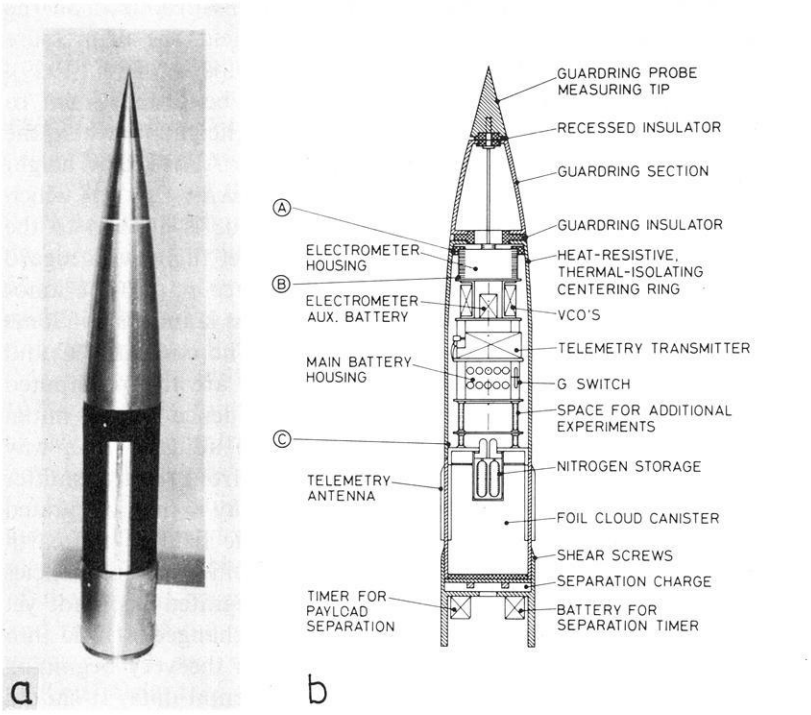

Fig. 5a and b. Actual design of payload B I left: photograph, right: schematic cross section (not to scale). Encircled letters refer to points where temperature measurements were taken

nose cone was at the bottom and through a temperature-insulating, thermal-resistant plastic centering ring at the top of the payload structure.

In order to suppress heat transfer by thermal convection, a number of small ventilating holes were drilled into the nose cone at its end. This ensured a rapid escape of air from the nose cone section during ascent.

The aerodynamic heating was however welcomed and used to advantage as a means of "natural" cleaning of the guard ring probe surface during ascent, especially of the nose tip. The nose tip was made as sharp as possible to assure attachment of the shockwave and to avoid any detachment which might otherwise cause problems in data interpretation.

Photocurrents were of no importance because their maximum value was for the worst case (the lowest heights) estimated to be of the order of one or two magnitudes less than the currents drawn from the environs.

A bay near the end of the ogival section of the nose cone was kept clear to provide space for experiments to be added in later projects (for example, Lyman-α and other radiation counters). On some flights, the space was used to house a modified Henderson probe (Henderson and Shiff, 1970) but despite very promising laboratory results, the probe behaved quite ambiguously during

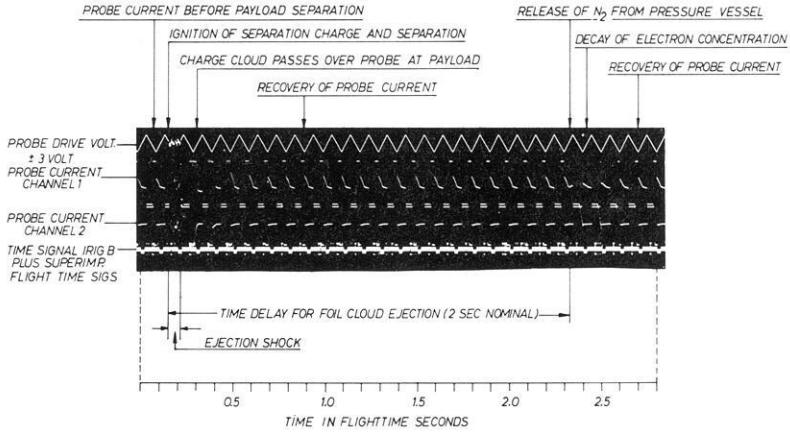

Fig. 6. Copy from telemetry record made on 35 mm film (photographic positive), which shows time interval between separation and foil expulsion. Data transmission for the guard ring probe is made over two separate subcarrier channels which transmit direct output of electrometer and output amplified by a factor of 10. Sensitivity of electrometer is alternatively changed by a factor of 100 at the peaks of the triangular probing waveform. By this, four order of magnitudes in current can be transmitted

flights. It was concluded that this approach to the measurement of atomic oxygen was not a reliable one and the probe was later abandoned.

The front end of the payload rested in a separation section to which it was tightly screwed on with shear screws. A flat, annular charge of explosive was fixed to the bottom of the ejection bay. It was fired at the apogee of the rocket's trajectory and separated the payload front end from the motor in order to expose the back end of the foil cloud canister. The explosive charge was 15 g of a stochiometric misture of potassium permanganate and magnesium powder. This composition had turned out to be superior in its characteristics and handling qualities in this special kind of application to conventional black-powder or double based grain powder charges.

1.8–2.2 s after separation pyrotechnic valves were opened for the release of compressed nitrogen which pushed out the foils, separated them, removed from the foils a considerable amount of centrifugal force and created the desired distribution inside the foil cloud. Separation of payload and ejection of foils is observable in the telemetry records of the guard ring probe as is shown in Figure 6: First, the ejection shock causes an interruption of the telemetry transmission which recovers after 80 ms. The cloud of combustion products and unburnt particles from the separation charge passes over the probe environment and causes a transient increase of electron concentration which is produced by photoemission of particles from the cloud. The moment of foil ejection is seen as a decrease in the electron concentration when the nitrogen cloud passes over the probe. These two events serve as simple housekeeping information about proper functioning of separation and foil cloud ejection.

Because the electronics of the payload is designed to stabilize within a few tenths of a second, no umbilical connector is required. Electric power to the payload electronics is applied when a simple inertia switch is actuated by the launch shock (motor ignition and initial acceleration). By this, the aerodynamic configuration of the rocket was kept clean, the design of the payload was simplified and hazards connected with the use of umbilicals on small rockets were avoided. The delay in response of the g-switch contributed to payload reliability because it is a common experience that electronic circuits can survive large shock loads when no power is applied. They often fail in the other case because transient short circuits and transient changes in component values that can occur under heavy g-load conditions may cause fatal overloads. The response time of the g-switch is set to such a value that it closes when the initial launch shock has passed.

Because the SKUA rocket is launched from a tubular launcher, there was some concern at the beginning that the probe surface might be contaminated by combustion products of the boost and sustainer propellant during the initial launch phase. Prototype flights and later experience have shown that this is not the case. The results of the prototype flights stressed however the necessity for a careful balancing of the payloads and led to some improvements of the final design too detailed to be described in this paper.

4. Some Results

Figure 7 illustrates how the circulation pattern of winds changes from winter to summer. High winter-anomalous absorption was observed only when westerlies are present in the whole height regime between 80 and 90 km. This indicates that this state is linked to a low-pressure system which has its center located north of the location where the measurements were made. Because we made our observations rather close to the time-variable southern border of the existence of winter-anomalous conditions, we saw more clearly than in more nothern latitudes that the winter-anomaly effect splits up into more than one period of high absorption. Between these events, extremely low absorption is observed in most cases. This raises the question how to define a "normal" and a "winter-anomalous" day. We tried to circumvent these difficulties by referring to electron concentration profiles which were measured at a time when both the wind field is calm and the absorption has little variation from day to day. This is mostly the case in the spring/early summer season.

Like Mechtly we found the maximum enhancement of electron concentration around 82 km (Dieminger et al., 1974). Since then more winter profiles of electron concentration became available. All were measured around local noon.

It takes no effort to classify these profiles either after similarity or after amount of absorption: in both cases, the profiles which sort into a group are the same. There are, however, some slight but significant differences between profiles belonging to the same group: Some of them have a higher electron concentration below about 78 km than others. This difference is related to the diurnal variation of absorption. The profile which has a higher electron

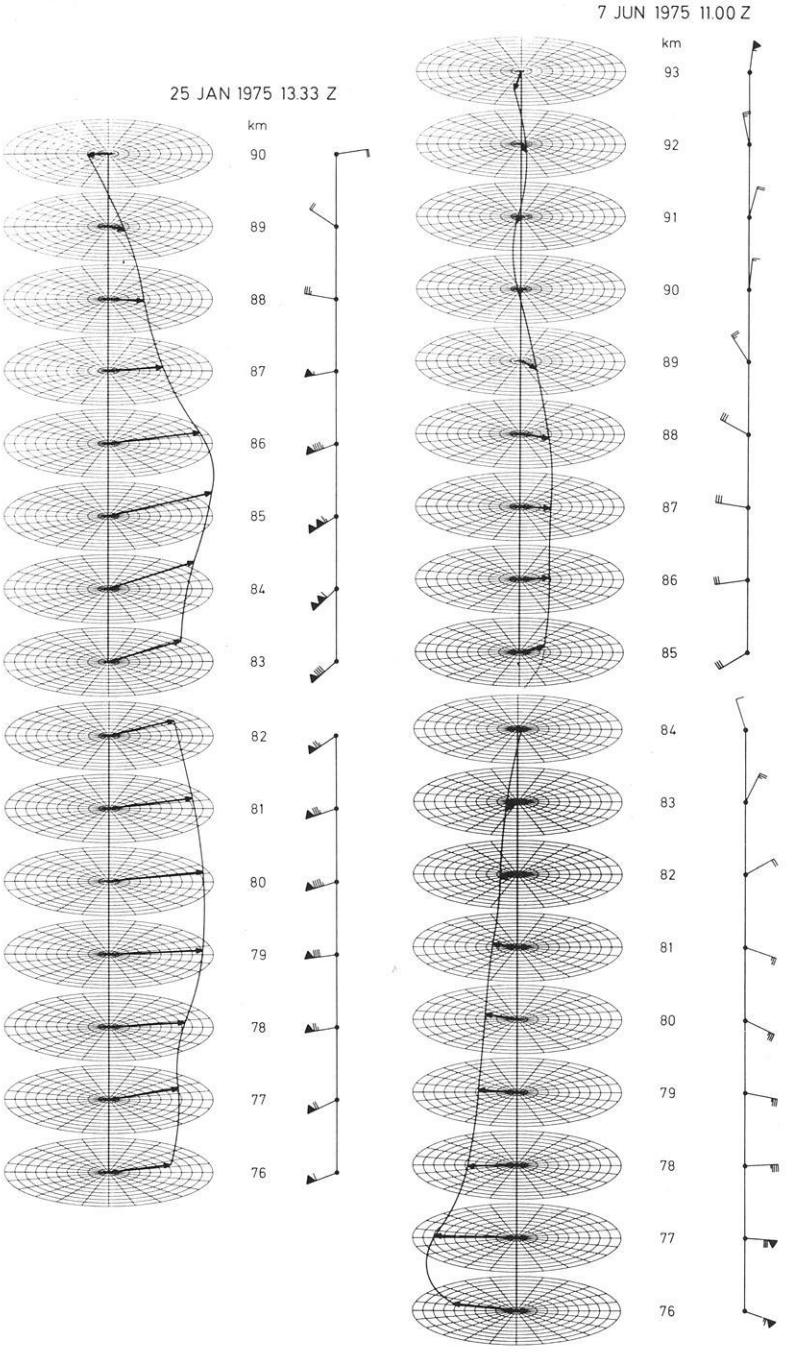

Fig. 7. Two Examples for wind measurements around noon time: Seasonal variation. *Left:* quasi-three dimensional "wind-band" presentation on compass cards. (North: top, west: left, east: right.) Each division: 10m/s. *Right:* meteorological "arrow" notation with barbs. The arrow is flying from where the wind is coming; speed indicated by barbs. One full triangular barb: 50 m/s; one light barb: 10 m/s, short barb: 5 m/s. Note the differences in speed and direction: Wind velocities in the 80–88 km region are much higher during winter

concentration in lower levels corresponds to a day for which the description of the diurnal variation of absorption by the $\cos^n\chi$-law is given by an "n" of the order of 1, while "n" is lower for the other profile. This difference is more clearly seen when the corresponding profiles of differential contribution to total absorption along the ray path $dL/dl \cdot \frac{1}{\cos\varphi}$ are considered. This is more closely related to the actual absorption measurement because it contains the electron collision frequency also. It is determined during the evaluation process of the guard ring probe results. For a comparison of different groups of absorption it is convenient to normalize the profiles of differential contribution to total absorption to the relevant amount of total absorption. When "n" has a high value (in the order of 1) a maximum contribution to absorption stems from the height region centered around 75 km (see Fig. 8). For lower "n" this maximum is shifted to greater heights above 78–80 km. This shift becomes pronounced when "n" is small (0.5 or less). This result can at least be qualitatively understood and related to composition changes in the D-region when model calculations made long time ago by Rawer (1943) are considered. He used a simplified model and assumed "thin" and "thick" absorbing layers (in the sense that their scale height was smaller than or equal to that of the environmental gas). He found that the diurnal variation of absorption is proportional to $\cos^{1/2}\chi$ when the layer is "thin" and the electron loss process is recombination. For attachment as the loss process, he arrived at $\cos\chi$. The corresponding values for a "thick" layers were $\cos^{1.5}\chi$ (recombination) and $\cos^2\chi$ (attachment). The simplifications made in this theory prevented its practical application in the past, but taking it as a guide and considering the results of our in-situ measurements, we can distinguish fairly clearly between at least two height levels which contribute to absorption. One level is below 78 km in which the electron loss process is, as is well known, the formation of negative ions. Above 80 km, the prevailing loss process during winter is recombination.

This level becomes more important when strong winter-anomalous conditions are present. However, there are exceptions in which both levels (above 80 and around 75 km) contribute about equally to total absorption and produce high winter-anomalous absorption. On such days, attachment in the lower level (or a loss process equivalent to attachment) governs the diurnal variation and yields a high "n" for the $\cos^n\chi$-approximation of the diurnal variation. Because the electron/ion ratio is extremely temperature-sensitive in these lower levels (Cipriano, Hale and Mitchell, 1974) one is tempted to relate these events to temperature increases (stratospheric warmings) but this has to be further investigated more closely.

Mass spectrometer results reported by Arnold and Krankowski (1971) and by Arnold, Kissel, Krankowski, Wieder and Zaehringer (1971) who found negative ions below 80 km but not in greater heights while Narcisi and co-workers (1972) did find them in heights between about 82 and 87 km but with a different composition fit well into this picture. These two results have been considered to be in conflict with each other but are less controversial if one considers the actual season and not the calendar date on which the two measurements were made and assumes that a depletion of water content in the D-region during winter is one of the main causes of winteranomaly.

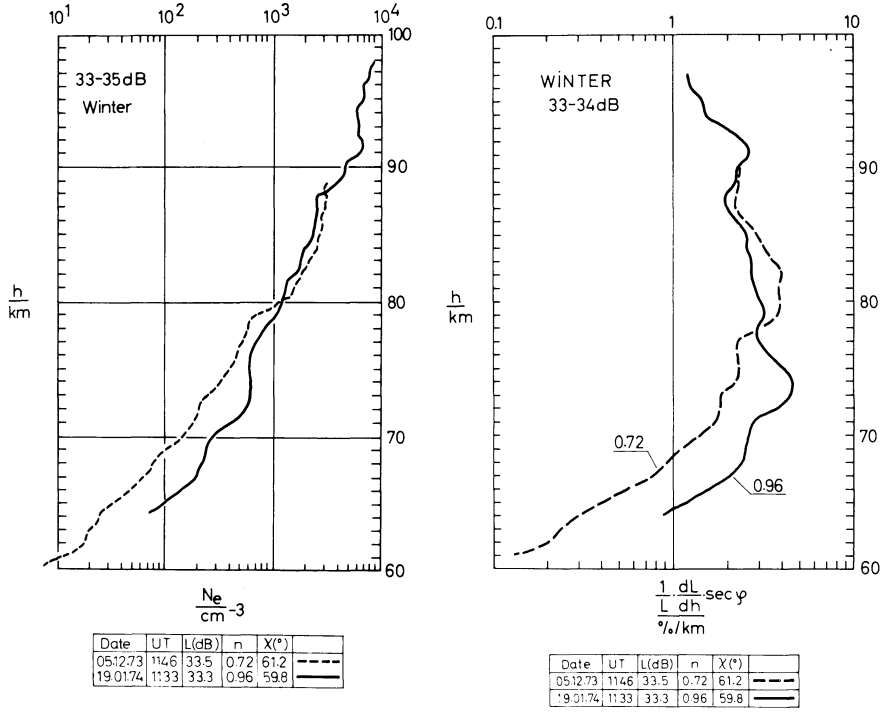

Fig. 8. An example for the relation between "n" of the $\cos^n\chi$ approximation of the diurnal variation of absorption and electron concentration profile resp. profile of differential contribution to total absorption along the ray path (the latter normalized to the relevant absorption value): When "n" is large, a maximum of contribution is found around 75 km (winter profiles)

Therefore, one of the things (amongst others) we want to learn from the results of other measurements taken in the Aeronomy Program is if there is a seasonal change in water vapor content and in the content of nitric oxide in the D-region, preferably between 78 and 88 km, because this would explain the disappearance or reduction of the ledge in electron concentration during winter conditions and the formation of the "bulge" of electron concentration found when high winter anomalous absorption is present.

Acknowledgement. The work was sponsored by the Bundesminister für Wissenschaft und Forschung (WRK 90) and, in part, by GRANT DAERO – 75-G-076.

Our sincere thanks go to our colleague Dr. A. Loidl who developed the probe electrometer and its associated circuity.

References

Arnold, F., Kissel, J., Krankowski, D., Wieder, H., Zaehringer, J.: Negative ions in the lower ionosphere: A mass-spectrometric measurement. J. Atmospheric. Terrest. Phys. **33**, pp. 1169–1175, 1971

Arnold, F., Krankowski, D.: Negative ions in the lower ionosphere: A comparison of model computation and a mass-spectrometer measurement. J. Atmospheric. Terrest. Phys. **33**, pp. 1693–1702, 1971

Azcarraga, A., Sanchez, L., Rose, G., Widdel, H.U.: An evaluation of the scale of mesospheric wind disturbances. In: Space Research, XII, pp. 613–614. Berlin: Akademie-Verlag 1972

Azcarraga, A., Sanchez, L., Widdel, H.U.: On the structure of mesospheric wind. In: Space Research, X, pp. 174–179. Amsterdam: North Holland Publ. Comp. 1970

Azcarraga, A., Sanchez, L., Widdel, H.U.: Measured wind oscillations at mesospheric levels. In: Space Research, XI, pp. 835–840. Berlin: Akademie-Verlag 1971

Borchers, R.: Untersuchungen der Eigenschaften einer Aspiration-Sonde (Gerdien-Kondensator) zur Bestimmung der Konzentrationen und Beweglichkeiten von Ladungsträgern beiderlei Vorzeichens im Höhenbereich zwischen 80 und 40 km. Forschungsbericht BMBW-FBW71-39, Bundesministerium für Bildung und Wissenschaften, 1971

Cipriano, J.P., Hale, L.C., Mitchell, H.D.: Relations among low ionosphere parameters and A_3 radio wave absorption. J. Geophys. Res. **79**, 2260–2265, 1974

Dieminger, W., Hoffman-Heyden, A.E.: Reflexionen von Kurzwellen aus Höhen unter 100 km. Naturwissenschaften **39**, 1, 1952

Dieminger, W., Rose, G., Widdel, H.U.: In situ measurements of electron concentration, neutral wind and air pressure compared with the winter anomaly. In: Lower ionosphere structure, K. Rawer, ed., pp. 341–348. Berlin: Akademie-Verlag 1974

Gregory, J.B.: Radio wave reflections from the mesosphere. I. Height of occurrence. J. Geophys. Res. **66**, 429–445, 1961

Henderson, W.R., Schiff, H.I.: A simple sensor for the measurement of atomic oxigen height profiles in the upper atmosphere. Planetary Space Sci. **18**, 1527–1534, 1970

Jones, L.M.: Upper air densities and temperatures from eight IGY rocket flights by the falling sphere method. WDC A, IGY R. Rep. No. 5, 1959

Mechtly, E.A.: Accuracy of rocket measurements of lower ionosphere electron concentrations. Radio Sci. **9**, 373–378, 1974

Mechtly, E.A., Shirke, J.S.: Rocket electron concentration measurements on winter days of normal and anomalous absorption. J. Geophys. Res. **73**, 6243–6247, 1968

Mechtly, E.A., Bowhill, S.A., Smith, L.G., Knoebel, H.W.: Lower ionosphere electron concentration and collision frequency from rocket measurements of Faraday rotation, differential absorption and probe current. J. Geophys. Res. **72**, 5239–5247, 1967

Narcisi, R.S., Bailey, A.D., Wlodyka, L.E., Philbrick, C.R.: Ion composition measurements in the lower ionosphere during November 1966 and March 1970 solar eclipses. J. Atmospheric. Terrest. Phys. **34**, 647–658, 1972

NASA-Sp-219: Status of passive inflatable falling-sphere technology for an atmospheric sensing to 100 km. Symposium Langley Res. Center, Hampton, Va. 23–24.9.1969. Office of Technology and Utilisation, NASA, Washington, D.C.

Otterman, J.: Analysis of a falling-sphere experiment for measurement of upper atmosphere density and wind velocity. J. Geophys. Res. **66**, 819–822, 1961

Pachomov, S.V.: Technique of obtaining data about winds in the mesosphere by small meteorological rockets. In: Small rocket instrumentation techniques, K.I. Maeda, ed., pp. 135–137. Amsterdam: North Holland Publ. Comp. 1969

Phelps, A.V., Pack, J.L.: Electron collision frequencies in nitrogen and in the lower ionosphere, Phys. Rev. Letters **3**, 240–342, 1959

Rapp, R.R.: The accuracy of wind derived by the tracking of chaff at high altitudes. J. Meteorol. **17**, 507–514, 1960

Rawer, K.: Der Einfluß der Dämpfung auf die Kurzwellenausbreitung. ZWBM Berlin-Adlershof, FB Nr. 1872, 1943

Rose, G., Weber, J., Widdel, H.U., Galdon, P.: Experimental results of radio wave absorption measurements in Southwest-Europe. In: Lower ionospheric structure, K. Rawer, ed., p. 331–339, Berlin: Akademie-Verlag 1974

Rose, G., Widdel, H.U.: Zur Möglichkeit des direkten Nachweises vertikaler Luftbewegungen in Höhenbereich 75–80 km. Z. Geophys. **35**, 211–212, 1969

Rose, G., Widdel, H.U.: On the possibility of a simultaneous measurement of wind spead, wind direction, air density and air temperatures at heights which correspond to the upper D-region (max 95 km) with chaff cloud sensors. Planetary Space Sci. **20**, 877–889, 1972

Rose, G., Widdel, H.U.: Results of air temperature, density and pressure measurements obtained with the aid of foil cloud sensors in the height region between 80 and 95 km. Planetary Space Sci. **21**, 1131–1140, 1973

Rose, G., Widdel, H.U.: D-region radio wave propagation experiments, their significance, and results during the Western European winter anomaly campaign 1975/76. J. Geophys. **44**, 15–2, 1977

Rose, G., Widdel, H.U., Azcarraga, A., Sanchez, L.: A payload for small sounding rockets for wind finding and density measurements in the height region between 95 and 75 km. Phil. Trans. Roy. Soc. London, A 271, 509–528, 1972a

Rose, G., Widdel, H.U., Azcarraga, A., Sanchez, L.: Experimental evidences for a transient ion layer formation in connection with sudden ionospheric disturbances in the height range 20–50 km. Planetary Space Sci. **20**, 871–876, 1972b

Rose, G., Widdel, H.U., Olsen, R.O., Kennedy, B.: Project "Limpas" ein Vergleich zwischen den Ergebnissen von Wind- und Dichtemessungen, gewonnen mit dem Verfahren „fallende Kugel" und dem Lindauer Folienwolken-Experiment. Kleinheubacher Berichte **19**, 471–482, 1976

Sechrist, C.F., Mechtly, E.A., Shirke, J.S., Theon, J.S.: Coordinated rocket measurements on the D-region winter anomaly – I. Experimental results. J. Atmospheric Terrest. Phys. **31**, 145–153, 1969

Smith, L.G.: The measurement of winds between 100.000 and 300.000 ft. by use of chaff rockets. J. Meteorol. **17**, 296–310, 1960

Smith, L.G.: Langmuir probes for measurements in the ionosphere. In: Electron density and temperature measurements in the ionosphere, K.I. Maeda, ed., pp. 2–31. revised edition, COSPAR Techniques Manual Series, 1967

Smith, L.G.: Langmuir probes in the ionosphere. In: Small rocket instrumentation techniques, K.I. Maeda, ed., pp. 1–15. Amsterdam: North Holland Publ. Comp. 1969

Thrane, E.V.: Ionospheric profiles up to 160 km – A review of techniques and profiles. In: COSPAR methods of measurement and results of lower ionosphere structure, K. Rawer, ed., pp. 3–21. Berlin: Akademie-Verlag 1974

Tiheridge, J.E.: The stratification of the lower ionosphere. J. Atmospheric. Terrest. Phys. **24**, 283–296, 1962

Webb, W.L.: The first meteorological rocket network. Bull. Am. Meteorol. Soc. **42**, 482–494, 1961

Widdel, H.U., Rose, G., Bordhers, R.: Results of concentration and mobility measurements of positively and negatively charged particles taken by a rocket-borne parachuted aspiration (Gerdien) probe in the height region from 72 to 39 km. Pageoph **84**, p. 154 160, 1971

Widdel, H.U., Rose, G., Borchers, R.: Payload B III – an instrument package for the measurement of conductivity, concentration and mobility of positive and negative ions in the mesosphere. J. Geophys. **43**, 179–188, 1977

Zimmerman, S.P., Narcisi, R.S.: The winter anomaly and related transport phenomena. J. Atmospheric. Terrest. Phys. **32**, 1305–1308, 1970

Received May 2, 1977; Revised Version June 6, 1977